Preprint BioRxiv

CST–Polymeraseα-primase solves a second telomere end-replication problem

Hiro Takai[1**], Valentina Aria[2**], Pamela Borges[1], Joseph T. P. Yeeles[2*], Titia de Lange[1*]

[1]Laboratory for Cell Biology and Genetics, Rockefeller University, New York, USA;

[2]Medical Research Council Laboratory of Molecular Biology, Cambridge, CB2, 0QH

*Correspondence to: Joseph T. P. Yeeles, email: jyeeles@mrc-lmb.cam.ac.uk

and Titia de Lange: delange@rockefeller.edu

** equal contribution

Telomerase solves the end-replication problem by adding G-rich telomeric repeats to the 3´ ends of telomeres[1]. We report a second end-replication problem affecting the C-rich telomeric repeat strand that is solved by fill-in synthesis by CST–Polymeraseα(Polα)-primase. *In vitro* replication of linear DNAs showed that lagging-strand DNA synthesis stops >40 nt before the replisome reaches the 5´ end of the template. Incomplete lagging-strand DNA synthesis is predicted to result in progressive shortening of the telomeric C-strand. Two assays to measure C-strand shortening at telomere ends in telomerase-deficient cells lacking the Ctc1 subunit of CST–Polα-primase revealed that lagging-end telomeres lose C-strand sequences at ~60 nt/population doubling (PD), consistent with the *in vitro* replication data. The C-strands of leading-end telomeres shortened by ~108 nt/PD, consistent with resection converting the blunt ends to 3´ overhangs. The overall shortening rate of the C-rich telomeric strand in Ctc1-deficient cells was consistent with the combined effects of incomplete lagging-strand synthesis and 5´ end resection at the leading-ends. We conclude that canonical DNA replication creates two telomere end-replication problems that require telomerase to maintain the G-rich strand and CST–Polα-primase to maintain the C-rich strand.

Main

Human telomeres are composed of long arrays of duplex TTAGGG repeats ending in a 3´ overhang of the G-rich strand (Fig. 1a). The 3´ overhang allows telomeres to adopt the protective t-loop configuration, which is thought to block ATM signaling and c-NHEJ at chromosome ends[2,3]. During the replication of telomeres, the C-rich 5´-ended strand

is the template for leading-strand DNA synthesis while the TTAGGG repeat strand templates lagging-strand DNA synthesis (Fig. 1a). The leading-strand product, presumed to be blunt, is processed by 5´ end resection to generate the 3´ overhang needed for t-loop formation and telomerase extension[4–7]. Indeed, human telomerase acts after DNA replication, extending the 3´ ends of both leading- and lagging-strand DNA synthesis products[8,9]. By extending the leading-end, telomerase can reconstitute the G-rich strand to the length of the parental telomere[10] (Fig. 1a). According to this scenario, telomerase is solely responsible for solving the telomere end-replication problem[7,10]. Lagging-strand synthesis was originally proposed to reach a point close to the 3´ end of the template, leaving a small gap after removal of the RNA primer used for Okazaki fragment synthesis[10] (Fig. 1a). Data on the structure of lagging-end telomeres in human cells suggested that synthesis of the last Okazaki fragment is initiated randomly along the 3´ overhang[11], but these priming events may have occurred during CST–Polα-primase fill-in synthesis as described below, rather than during canonical DNA replication. Here we use an *in vitro* DNA replication system to determine priming sites for the last Okazaki fragment generated by the replisome and identify an additional end-replication problem that it is solved by CST–Polα-primase *in vivo*.

To determine how the replisome behaves at the end of a linear DNA template, we utilized an *in vitro* reconstituted DNA replication system to map 5´ ends of nascent lagging- and leading strands (Fig. 1b-e). In this system, replisomes are assembled with purified *Saccharomyces cerevisiae* proteins that perform complete leading and lagging-strand replication at the *in vivo* rate[12,13]. Origin-dependent DNA replication was performed on linear templates that either carried a 100 nt 3´ overhang or no overhang

(Fig. 1c). Prior to analysis through denaturing polyacrylamide gels, the radiolabelled replication products were nicked with Nb.BbvCI or Nt.BbvCI which liberate nascent lagging- and leading-strand ends, respectively (Fig. 1b,c). In this setting, the 3´ end of the leading strand was uniformly extended to the end of the template resulting in a single Nt.BbvCI product of the expected size (236 and 336 nt for templates with and without overhang, respectively), establishing that leading-strand DNA synthesis efficiently completes the replication of a linear DNA, as predicted by data on yeast telomere replication[14,15]. The data demonstrate that lagging-strand synthesis terminates within a broad region up reaching as far as ~150-200 nt from the end of the duplex region of the template. Strikingly, after RNase HII digestion, the longest RNase HII sensitive lagging-strand DNA products were at least 40 nt shorter than the corresponding leading-strand products regardless of the presence of a 3´ overhang (Fig. 1d, e; Extended Data Fig. 1a, b). These results reveal that the core eukaryotic replisome is unable to initiate new Okazaki fragments once it gets to within ~30 nt of the end of the leading-strand template and consequently cannot sustain canonical lagging-strand synthesis along a 3´ overhang (Fig. 1f). This behaviour is consistent with recent cryo-EM structures of yeast and human replisomes containing Polα-primase[16]. In both structures, the primase active site is positioned ~75 Å from the point of template unwinding, which equates to ~20-30 nucleotides of single-stranded (ss) DNA (Extended Data Fig. 1c). Consequently, in this configuration, Polα-primase is unable to prime within the last ~30 nt of a linear template because the parental DNA duplex will be fully unwound before the template has reached the primase active site. Moreover, because the positioning of Polα-primase in the replisome is highly conserved between budding

yeast and human (Extended Data Fig. 1c), it is reasonable to expect that lagging-strand replication by human replisomes will display the same behave as budding yeast replisomes during the duplication of telomeres. Due to this additional end-replication problem, the C-rich telomeric strand is predicted to continuously shorten by >40 nt and this shortening will not be mitigated by extension of the G-rich strand by telomerase.

Sequence loss from the 5´ end of the C-rich telomeric strand can be counteracted by Polα-primase in association with the CST (Ctc1, Stn1, Ten1) complex[17,18]. CST is an RPA-like ssDNA binding protein that interacts with Polα-primase, stimulating the activity and increasing the processivity of Polα[19–28]. At mammalian telomeres, CST–Polα-primase can fill in telomere ends that have been hyper-resected, thereby preventing excessive telomere shortening[4,5,29,30]. Prior work has shown that the C-rich strand progressively shortens when CST–Polα-primase fill-in is disabled[29,30] but the rate of shortening and its cause were not determined.

We set out to determine whether lagging-strand DNA synthesis results in shortened C-strands *in vivo*. CsCl-gradients can be used to separate telomeres generated by leading- and lagging-strand DNA synthesis based on their differential incorporation of BrdU[11] (Extended Data Fig. 2a). This method yields very low amounts of DNA, necessitating quantification of the 3´ overhangs by the sensitive in-gel hybridization method[4,31]. We applied this approach to CTC1$^{F/F}$ HCT116 cells[29] from which *CTC1* can be deleted upon induction of Cre with tamoxifen (4-OHT). CTC1$^{F/F}$ cells express telomerase but were rendered telomerase-negative through bulk CRISPR/Cas9 KO of hTERT and further inhibition of telomerase activity with BIBR1532[32] so that no extension of the 3´ overhangs by telomerase will take place (Fig.

2a-d). The relative 3´ overhang signals from six independent experiments showed that deletion of *CTC1* induced a substantial increase in the relative 3´ overhang signals at both leading- and lagging-end telomeres, as expected from prior work[4,5,29,30] (Fig. 2c,d).

Because the in-gel detection of telomeric overhangs yields only relative values, we aimed to determine the absolute length of the 3´ overhang in at least one of the samples so that the relative overhang values from the in-gel assays could be calibrated. We developed two methods to measure absolute lengths of the 3´ overhang in untreated cells containing wild type CST in the presence or absence of telomerase activity (Fig. 2e-h; Extended Data Fig. 3). The first method, inspired by primer extension experiments performed with yeast and human telomeric DNA[31,33], is based on a PCR amplification of a fill-in product generated with the 3´ overhang as a template (Extended Data Fig. 3a). This method relies on poly(A) tailing of the 3´ ends of the telomeres, annealing of a set of oligodT-containing primers that can anneal to each of the six possible 3´ end sequences of telomeres, and extension of the primers with Q5 and T4 polymerase. The oligodT primers also contained a specific sequence for PCR (Teltail) and a 5´ Biotin allowing isolation of the extension products. The extension products are tailed with rGTP and ligated to an adapter allowing generation of PCR products that are analyzed on blots of polyacrylamide/urea gels hybridized to a radiolabelled G-strand oligonucleotide. The method was tested on a telomere model substrate featuring a stretch of duplex telomeric repeats and a [TTAGGG]n 3´ overhang of 56 nt (Extended Data Fig. 3b,c). This substrate yielded a PCR product of the expected length that was not observed when the 3´ overhang was removed with the *E. coli* 3´ exonuclease ExoI (Extended Data Fig. 3c).

DNA from Ctc1-proficient cells resulted in ladders of products that were largely absent when the DNA was first treated with ExoI to remove the 3´ overhangs (Fig. 2e; Extended Data Fig. 3d,e). As is the case for the PCR products in Single Telomere Length Analysis (STELA[34]), individual PCR reactions on the same sample yielded different sets of bands, indicating that each band is likely represents the 3´ overhang of a single telomere. Control experiments with oligos designed to represent fill-in products from 3´ overhangs with 5-15 repeats indicated that the assay was robust, yielding products with the expected length and intensity (Extended Data Fig. 3f,g). An oligo representing 20 repeats was also readily detected although with greater variation in intensity (Extended Data Fig. 3g). Using this approach, the lengths of the 3´ overhangs in genomic DNAs from $CTC1^{F/F}$ and $CTC1^{F/F}$ sgTERT/BIBR1532 cells (neither treated with 4-OHT) was measured (Fig. 2f; Extended Data Fig. 3g). Results obtained with four independent DNA preparations (four PCR reactions for each DNA sample) revealed that the 3´ overhangs were on average 89 and 84 nt in cells with and without telomerase, respectively. The similar 3´ overhang lengths in the two sets of cells is consistent with data from in-gel hybridization experiments which showed a minimal difference in their relative 3´ overhang signals (Extended Data Fig. 3h). As expected, the 3´ overhang PCR products were substantially longer after deletion of Ctc1 (Extended Data Fig. 3e).

In an orthogonal approach to determine the absolute length of the 3´ overhang, we measured the shortening of the G-rich telomeric strand upon removal of the 3´ overhangs with ExoI. This method is reminiscent of experiments done on yeast telomeres, which are sufficiently short to be analyzed by PCR before and after ExoI treatment[14]. To analyze the longer telomeres of HCT116 cells, genomic DNA was

treated with ExoI, digested with MboI and AluI to generate telomeric restriction fragments, and the reduction in the size of the telomeric G-strand was measured on alkaline agarose gels by in-gel hybridization. This method was tested on the model telomere with a 3´ overhang of defined length (Extended Data Fig. 3b). ExoI digestion of the linear DNA with the 3´ overhang reduced the size of the G-strand DNA by 57 nt which is close to the expected value of 56 nt (Extended Data Fig. 4a). The ExoI method was applied to DNA from Ctc1-profient cells with and without telomerase (Fig. 2g,h; Extended Data Fig. 4b,c), which showed 3´ overhang lengths for cells with and without telomerase of 90 and 80 nt, respectively (Fig. 2h). These values are close to those obtained by the PCR method.

The overhang lengths determined by the PCR and ExoI methods were used to calibrate the data on relative overhang signals measured on separated leading- and lagging-end telomeres from cells with and without Ctc1 (Fig. 2i). According to this analysis, telomerase-negative cells lacking Ctc1 have 3´ overhangs of ~110 and ~220 nt at their leading- and lagging-end telomeres, respectively. Taking these values into account, our modelling (Extended Data Fig. 5) indicates that the leading-end telomeres lose 105-110 nt of C-rich sequences due to resection while the lagging-end telomeres lose 59-62 nt. The finding of ~60 nt C-strand loss at lagging-end telomeres is consistent with the loss of >40 nt predicted from the *in vitro* analysis of the lagging-end replication products. We cannot exclude that the loss of C-strand sequences from the lagging-end telomeres is due to exonucleolytic attack, rather than a lagging-strand replication deficiency. However, we consider this possibility unlikely because it would require a regulatory mechanism that leads to distinct outcomes of resection at the leading- and

lagging telomere ends. Furthermore, a previous study showed that no resection occurred at lagging-end telomeres in human cells[11], although lagging-end resection was observed in mouse cells[4].

Based on the inferred average C-strand shortening caused by resection at the leading-ends (108 nt) and incomplete synthesis at the lagging-ends (60 nt) (Fig. 2j), we predicted how the length of the 3´ overhang will change with cell divisions when Ctc1 is absent from telomerase-negative cells (Fig. 3a; Extended Data Fig. 5). We then measured the relative normalized 3´ overhang signals in telomerase-negative cells from which *CTC1* was deleted using the in-gel overhang assay (Fig. 3b). The graph of the results from three independent experiments was nearly identical to the predicted relative overhang change (Fig. 3c).

To further test whether the shortening of telomeric DNA *in vivo* is consistent with the predictions in Fig. 2i, we examined how the G- and C-rich strands changed with cell divisions after *CTC1* deletion from telomerase-positive cells (Fig. 4a,b; Extended Data Fig. 6a,b). The G-strand was rapidly extended by ~200 nt/PD when *CTC1* was deleted, consistent with the lack of inhibition of telomerase by CST (Fig. 4a-c; Extended Data Fig. 6a-c; Extended Data Fig. 7). While the G-strand elongated, the C-strand shortened, confirming the finding that, *in vitro*, the replisome is incapable of initiating Okazaki fragment synthesis on the 3´ overhang. Based on the inferred rate of C-strand sequence loss at the lagging- and leading-end telomeres, the overall rate of C-strand shortening is predicted to be ~84 nt/PD, which is close to the observed rate of C-strand shortening (Fig. 4d; Extended Data Fig. 6c).

The data reported here indicate that DNA replication creates a dual problem at telomere ends (Fig. 4e). The results of *in vitro* replication verify the long-held view that leading-strand replication leads to loss of the G-rich 3´ overhang sequence at one daughter telomere, representing the end-replication problem that can be solved by telomerase. We document a second end-replication problem *in vitro* and *in vivo* that results from the inability of lagging-strand DNA synthesis to synthesize a C-strand of the same length as the parental C-strand (Fig. 4e). Our data indicate that CST–Polα-primase counteracts this C-strand loss through fill-in synthesis at lagging-end telomeres. CST–Polα-primase-mediated fill-in also mitigates C-strand loss at the leading-end telomeres where resection generates the 3´ overhang used by telomerase[4,5,29,30] (Fig. 4e). Together these processes shorten the telomeric C-strand by approximately 84 nt/PD in HCT116 cells. In keeping with the critical role of CST–Polα-primase in solving the second end-replication problem, defects in this pathway result in severe human diseases (reviewed in refs. 18 and 35[18,35]). It was proposed that CST–Polα-primase evolved in LECA (or its Asgard archaeal ancestor) to maintain the 5´ ends of linear chromosomes[18,22]. Our data argue in favor of this view since the lagging-strand end-replication problem likely threatened the maintenance of the first linear chromosomes.

Methods

Construction of replication templates

In vitro replication assays to map the 5´ end of the lagging strand were performed on SapI-linearized vVA25 (blunt) and a derivative containing a 100 nt 3´ overhang. To construct vVA25, a single BbvCI site was inserted ~ 200 nt upstream of the SapI site in vVA22 [15]. Plasmid DNA was purified by CsCl density gradient centrifugation before linearization with SapI.

To generate the 3´ overhang template, a 25 bp duplex with a 100 base 3´ overhang was generated by annealing oligos VA67 (Sigma) and 3´-overhang (IDT). Annealed oligos were ligated onto SapI-linearized vVA25. The ligation (400 μl) was performed overnight at 16°C in 1x T4 Ligase buffer (New England Biolabs (NEB)) supplemented with 5 mM $Mg(OAc)_2$, 62.5 nM SapI-linearized vVA25, 2.5 mM 25 bp duplex with 100 base 3´ overhang and 23,800 units T4 Ligase (NEB). Unligated oligonucleotides were removed by gel filtration through a 50 cm x 0.7 cm Sepharose 4B column (Sigma) equilibrated in 5 mM Tris-HCl pH 8, 0.1 mM EDTA.

Standard replication reaction

Standard replication reactions were carried out as reported previously (Aria and Yeeles, 2019) with minor alterations. MCM loading and phosphorylation reaction was performed in a reaction (80 μl) containing: 25 mM Hepes-KOH, pH 7.6; 100 mM potassium glutamate; 0.01% NP-40-S; 1 mM DTT; 10 mM $Mg(OAc)_2$; 0.1 mg/ml BSA; 3 mM ATP; 2.5 mM DNA template; 75 nM Cdt1-Mcm2-7; 40 nM Cdc6; 20 nM ORC; 25 mM DDK.

After incubation at 30°C for 20 minutes, the loading reaction was 2-fold diluted in replication buffer. The final concentrations of the components are: 25 mM Hepes-KOH, pH 7.6; 250 mM potassium glutamate; 0.01% NP-40-S; 1mM DTT; 10 mM $Mg(OAc)_2$; 0.1 mg/ml BSA; 2 mM ATP; 0.2 mM GTP; 0.2 mM CTP; 0.2 mM TTP; 0.2 mM UTP; 30 μM dATP; 30 μM dTTP; 30 μM dCTP; 30 μM dGTP; 1 μCi [α-^{32}P]-dCTP. Replication was initiated by adding the following concentrations of the following factors: 30 nM Dpb11; 100 nM GINS; 30 nM Cdc45; 10 nM Mcm10; 20 nM Ctf4; 20 nM Csm3/Tof1; 20 nM RFC; 20 nM PCNA; 20 nM Pol ϵ; 10 nM Pol δ; 100 nM RPA; 20 nM Pol α; 10 nM Topoisomerase I; 25 nM S-CDK; 20 nM Cdc9; 20 nM Fen1; 10 nM Mrc1; 12.5 nM Sld3/7; 30 nM Sld2. After 60 minutes at 30℃, the reaction was stopped with a final concentration of 50 mM EDTA and the proteins were removed by treatment with proteinase K (1/100 of the volume – NEB) and SDS (0.1%) for 15 minutes at 37℃. The DNA was extracted with phenol-chloroform-isoamyl alcohol (Sigma-Aldrich) and unincorporated nucleotide removed with Illustra G-50 columns (GE Healthcare).

To map the 5´ end of the end of the lagging-strand product and the 3´ end of the leading-strand product of rightward moving replication forks, reaction products were digested with either Nt.BbvCI (leading strand) or Nb.BbvCI (lagging strand) (0.025 U/μl) for 10 min at 37℃. Reactions were stopped with EDTA, deproteinized and the DNA extracted, as described above, before analysis through 1% alkaline agarose gels. Samples were further analyzed by denaturing polyacrylamide electrophoresis. For this analysis, DNA was ethanol-precipitated, resuspended in 10 mM Tris-HCl, pH 8.0; 1 mM EDTA and either digested or mock-treated with RNase HII (NEB) for 1 hour at 37°C in 1x ThermoPol buffer (NEB). Samples were processed and analyzed as described[15].

Oligos used for generation of DNA termini: VA67, 5´-TAGTCCATCGGTTTTGCCATAAGAC-3 ‘; 3´ overhang, 5´-GCTGTCTTATGGCAAAACCGATGGACTATGTTTCGGGTAGCACCAGGAGTCTGTAGCACGTGCATCTCAACGTGGCGTGAGTACCTTTTAATCACCGCTTCATGCTAAGGATCTGGCTGCATGCTATG-3´.

Cell culture and immunoblots

Culturing of CTC1$^{F/F}$ HCT116 cells and *CTC1* deletion by induction of Cre with 4-hydroxytamoxifen (4-OHT) was performed as described[29]. Ctc1 loss was verified by immunoblotting using rabbit polyclonal antibody raised against full length recombinant human Ctc1 (a gift from John C. Zinder) as described[36]. CTC1$^{F/F}$ cells were rendered telomerase deficient by bulk targeting of hTERT with lentiCRISPR v2 vector expressing Cas9 and sgRNAs (5´-ACACGGTGACCGACGCACTG-3´ and 5´-CTTGGTCTCGGCGTACACCG-3´). Telomerase was further inhibited using 16 μM BIBR1532[32] (TOCRIS #2981) in the media. TRAP assays for telomerase activity were done using the TRAPeze kit (Millipore, #S7700) according to the manufacture’s instruction.

Overhang analysis of leading- and lagging-end telomeres

Isolation of genomic DNA and separation of leading- and lagging-end telomeres were performed as described[4,11]. Briefly, cells were cultured with 100 μM BrdU for 16 h, harvested, and genomic DNA was extracted. DNAs were fractionated on CsCl density gradients and fractions were collected from the bottom of the centrifuge tubes.

Telomeric DNA in each fraction was quantified by slot blot hybridization using γ-^{32}P-ATP end-labeled $[TTAGGG]_4$ (TelG probe) as described[4]. Leading- and lagging-end peak fractions were pooled, dialyzed to remove most CsCl, and DNAs were isolated by ethanol precipitation followed by suspension in TE. The pooled fractions were analyzed by agarose in-gel overhang analysis with a γ-^{32}P-ATP end-labeled $[AACCCT]_4$ (TelC probe) as described[4].

PCR assay for telomeric overhang (Method I)

$2x10^6$ cells were trypsinized, pelleted, frozen in liquid N_2, and stored at -80ºC. For DNA extraction, the cell pellet was resuspended to 1 ml TLE buffer (10 mM Tris-HCl pH 7.8, 100 mM LiCl, 10 mM EDTA, and 100 ug/ml RNAse A (Sigma, #R5000). 1 ml TLES buffer (TLE + 0.1% (w/v) SDS) with 100 ug/ml proteinase K (Roche, #03115879001) was added and the suspension was incubated at 37ºC for 10 min. Genomic DNA was extracted with 2 ml phenol-chloroform-isoamyl alcohol (Thermo Fisher, #BP1752I), followed by DNA precipitation with 1/20 volume of 8 M LiCl and 1 volume of isopropanol. Genomic DNA was resuspended in 50 μl TE buffer containing 50 mM LiCl (50 mM LiCl-TE), 100 ug/ml RNAse A, and 0.2 U/μl RNAse H (NEB #M0297) and immediately used for the overhang assay as follows. Genomic DNA (30 μl) was poly(A) tailed using 20 units terminal transferase (TdT, NEB, #M0315) and 0.2 mM dATP for 15 min at 37ºC in TdT buffer (20 mM Tris-HCl pH 7.9, 50 mM LiCl, 10 mM $MgCl_2$), followed by phenol-chloroform extraction and isopropanol precipitation as above. DNA was resuspended in 40 μl Extension buffer (10 mM Tris-HCl pH 7.9, 50 mM LiCl, 10 mM $MgCl_2$, and 50 μg/ml BSA). The tailed DNA was annealed to 0.2 nM 5´ biotinylated teltail ss-adaptor at

21ºC for 10 min, primer extension was performed with 0.006 U/μl Q5 (NEB, #M0491) and 200 μM each of dATP/dCTP/dTTP at 21ºC for 10 min and an additional 15 min incubation with 25 nM recombinant human RPA (a gift from Sarah W. Cai) and 0.03 U/μl T4 DNA polymerase (NEB, #M0203) at 37ºC. The teltail ss-adaptor (see below) is a mixture of single-strand DNA oligos of 5´ biotinylated teltail[34] followed by $[T]_8$ and 4 nt of C-strand sequence in 6 permutations. Extended DNA was digested with AluI at 37ºC for 20 min to diminish the viscosity. Excess teltail ss-adaptor and short bulk genomic DNA fragments were removed by DNA size selection using 25 μl SPRI select (Beckman, 0.5x v/v SPRI beads to DNA suspension). After 2 washes with 80% EtOH according to the manufacturer's instructions, DNA was eluted in 60 μl TE buffer and the concentration of DNA was measured using NanoDrop (Thermo Fisher). 0.5 μg DNA was used for the subsequent steps. After capture of the products on washed Streptavidin beads (10 μl, Dynabeads M-280, Thermo Fisher, #11205D), the DNA was denatured with 150 mM NaOH for 5 min at 21ºC 2 times, neutralized by 2 washes with 1 M LiCl-TE buffer, one wash with 50 mM LiCl-TE, and resuspended in 50 μl TdT buffer containing 2 mM rGTP (Promega, E603B) and 20 U TdT at 37ºC for 15 min for rGTP tailing[37]. DNA-bound beads were rinsed 3 times with 50 mM LiCl-TE and ligated to P1 ds-adaptor for >1 h at 21ºC in Ligation mix (Extension buffer containing 20 nM P1 ds-adaptor, 200 μM ATP, 25% PEG 8000, 8 U/μl Salt-T4 DNA ligase (NEB #M0467)). P1 ds-adaptors are double-strand (ds) splint adaptors that contain 5´-overhang with the 6 permutations of the telomeric sequence (see below). 6 permutated upper-oligos and the 5´ phosphorylated lower-oligo were mixed, annealed, and kept as aliquots at -20ºC to avoid multiple

freeze-thaw cycles. After 2 washes with 1 M LiCl-TE buffer, DNA-bound beads were resuspended in 20 μl TE buffer.

PCR with the teltail and P1 PCR primers was performed using Q5 PCR enzyme mix (NEB, #M0494) and the following conditions using 0.1 μl DNA-bound beads: denaturation at 98ºC for 30 sec; 30 cycles of 10 sec at 98ºC, 20 sec at 69ºC, and 50 sec at 72ºC; final extension for 5 min at 72ºC. PCR products were denatured at 80ºC for 5 min in 2x loading buffer (95% Formaldehyde, 10 mM EDTA, 0.05% xylene cyanol, and 0.05% bromophenol blue) and separated on 4.5% polyacrylamide/7 M urea gels in 1xTBE buffer and electroblotted in 0.5xTBE onto nylon membranes (Hybond-N^+, Cytiva). DNA was UV-crosslinked to the membranes, hybridized with γ-^{32}P-ATP end-labeled $[TTAGGG]_4$ (TelG probe) in Church mix at 48ºC and washed in 4x SSC/0.1% SDS at 48ºC.

For PCR assay with synthetic telomeric oligos $[TTAGGG]_{5\text{-}20}$-TTAG-$[A]_{10}$, 20 pM ss-oligo DNA was used for primer extension. The Poly(A) tailing, AluI digestion, and DNA size selection steps were skipped. The standard curve was generated using GraphPad Prism software (Dotmatics, ver.10).

Oligonucleotides for the PCR method

Oligonucleotides were synthesized by IDT or Thermo Fisher with indicated modifications and purification on PAGE.

The teltail ss adaptors 1-6 used for extension were as follows (telomeric sequences underlined). Adaptor 1: 5´-[5biotin]- TGCTCCGTGCATCTGGCATC TTTTTTTT <u>CTAA</u>-3´; adaptor 2: as adaptor 1 but ending in <u>TAAC</u>-3´; adaptor 3: as

adaptor 1 but ending in AACC-3´; adaptor 4: as adaptor 1 but ending in ACCC-3´; adaptor 5: as adaptor 1 but ending CCCT-3´; adaptor 6: as adaptor 1 but ending in CCTA-3´.

The P1 ds adaptors upper 1-6 oligonucleotides were as follows (telomeric sequences underlined). Upper 1: 5´-[5AmMC6]- GCACAGCCACTGGTAACG CCC GGTTAG-[3AmC7]-3´; upper 2, as upper 1 but ending in GTTAGG-[3AmC7]-3´; upper 3: as adaptor 1 but ending in TTAGGG-[3AmC7]-3´; upper 4: as adaptor 1 but ending in TAGGGT-[3AmC7]-3´; upper 5: as adaptor 1 but ending in AGGGTT-[3AmC7]-3´; upper 6: as adaptor 1 but ending in GGGTTA-[3AmC7]-3´. The P1 ds adaptor lower was: 5´-[5phos]-CGTTACCAGTGGCTGTGC-[3ddC]-3´.

PCR was performed with the following primers. Teltail primer: 5´-TGCTCCGTGCATCTGGCATC-3´; P1 primer: 5´-GCACAGCCACTGGTAACG-3´

The following control oligos were used to test the assay. Tel5-TTAG-A10: 5´-[TTAGGG]$_5$TTAG AAAAAAAAAA-3´; Tel10-TTAG-A10: 5´-[TTAGGG]$_{10}$TTAG AAAAAAAAAA-3´; Tel15-TTAG-A10: 5´-[TTAGGG]$_{15}$TTAG AAAAAAAAAA-3´; Tel20-TTAG-A10: 5´-[TTAGGG]$_{20}$TTAG AAAAAAAAAA-3´.

Generation of the model telomere substrate

A model telomere substrate containing a 56 nt 3´ telomeric overhang was constructed using BglII-linearized pSXneo1.6T_2AG_3[38]. To generate the 3´ overhang, 1 μM 5´-CTAACCCTAAGCTCTGCGACAT -3´ and 5´- GATCATGTCGCAGAGC[TTAGGG]$_{11}$ -3´ were phosphorylated with T4 polynucleotide kinase, annealed, and incubated with 0.1 μM linear pSXneo1.6T2AG3. Ligation was done in the presence of BglII with 6

cycles at 37ºC for 5 min and 21ºC for 5 min. The ligated product was gel purified on a 1% agarose gel.

ExoI digestion

Genomic DNA (2 μg) or the model telomere substrate was incubated with 40 U *E. coli* ExoI (#M0293, NEB) in 67 mM Glycine-NaOH (pH 9.5), 6.7 mM $MgCl_2$ and 10 mM 2-mercaptoethanol at 37ºC for >6 h (or overnight). After ExoI digestion, DNA was purified by phenol-chloroform extraction and isopropanol precipitation and used for the PCR assay for telomeric overhang analysis. For in-gel telomere hybridization assay, genomic DNA was digested with MboI and AluI after the ExoI treatment.

Telomeric overhang measurement using ExoI (Method II)

In method II, genomic DNA was treated (or not) with *E. coli* ExoI. After ExoI or mock treatment, DNAs were precipitated, digested with MboI and AluI, fractionated on 0.7% alkaline gels, and after neutralization (twice for 15 min in 0.5 M Tris-HCl (pH 7.0)/3 M NaCl) gels were dried and hybridized with end-labelled TelC. Gels were scanned and the average size of the fragments was calculated taking into account that the hybridization intensity increases with fragment length; mean TRF length = $\Sigma(SI_i)/\Sigma(SI_i / MW_i)$, where SI is the signal intensity at position *i* and MW_i is the TRF length at that position[39].

As a control, pSXNeo1.6T2AG3[38] was digested with HindIII and BglII, ligated (or not) to an oligonucleotide bearing a telomeric 3´ overhang of 56 nt (as described above for the model telomere substrate), and the 3 kb fragments with and without the

overhang were purified from agarose gel. The DNA fragments were treated (or not) with 20 U of *E. coli* ExoI, processed on alkaline gels as above, and detected by in-gel hybridization with the TelC probe.

Alkaline gel analysis of the telomeric G- and C-strands

Genomic DNA from was digested with MboI and AluI and denatured in 50 mM NaOH and 1 mM EDTA before fractionating the DNA on 0.7% alkaline agarose gels as described[40]. Gels were neutralized in 0.5 M Tris-HCl (pH 7.0)/3 M NaCl. Gels were dried, prehybridized in Church mix for 1 h at 50ºC, and hybridized overnight at 50ºC in Church mix with γ-^{32}P-ATP end-labeled $[AACCCT]_4$ (TelC) or $[TTAGGG]_4$ (TelG) as described[4].

Author contribution

H.T. and T.d.L. conceived and designed the study. A.V. and J.T.P.Y. designed and performed the in vitro replication experiments. All in vivo experiments were executed by H.T. with help from P.B. in the early stages of the project. T.d.L. wrote the manuscript with input from all authors.

Acknowledgements

We thank Carolyn Price for providing the CTC1$^{F/F}$ HCT116 cell line. We thank the members of the de Lange lab for comments on this work, Viviana Risca and Andres Mansisidor for advice on the PCR method, John C. Zinder for the Ctc1 antibody, and Sarah Cai for purified human RPA. This work is supported by grants from the NCI

(R35CA210036), the NIA (RO1AG016642), and the BCRF to TdL; a grant from the NCI to HT (5R50CA243771-02); and a grant to JTPY from the Medical Research Council (No. MC_UP_1201/12).

Conflict of interest

TdL is a member of the Scientific Advisory Board of Calico Life Sciences LLC, San Francisco

Refences

1. Greider, C. W. & Blackburn, E. H. Identification of a specific telomere terminal transferase activity in Tetrahymena extracts. *Cell* **43**, 405-413 (1985).
2. Griffith, J. D., Comeau, L., Rosenfield, S., Stansel, R. M., Bianchi, A., Moss, H. & de Lange, T. Mammalian telomeres end in a large duplex loop. *Cell* **97**, 503-514 (1999).
3. Doksani, Y., Wu, J. Y., de Lange, T. & Zhuang, X. Super-resolution fluorescence imaging of telomeres reveals TRF2-dependent T-loop formation. *Cell* **155**, 345-356 (2013).
4. Wu, P., Takai, H. & de Lange, T. Telomeric 3' overhangs derive from resection by Exo1 and Apollo and fill-in by POT1b-associated CST. *Cell* **150**, 39-52 (2012).
5. Wang, F., Stewart, J. A., Kasbek, C., Zhao, Y., Wright, W. E. & Price, C. M. Human CST has independent functions during telomere duplex replication and C-strand fill-in. *Cell Rep* **2**, 1096-1103 (2012).
6. Dai, X., Huang, C., Bhusari, A., Sampathi, S., Schubert, K. & Chai, W. Molecular steps of G-overhang generation at human telomeres and its function in chromosome end protection. *EMBO J* **29**, 2788-2801 (2010).
7. Stewart, J. A., Wang, Y., Ackerson, S. M. & Schuck, P. L. Emerging roles of CST in maintaining genome stability and human disease. *Front Biosci (Landmark Ed)* **23**, 1564-1586 (2018).

8. Zhao, Y., Sfeir, A. J., Zou, Y., Buseman, C. M., Chow, T. T., Shay, J. W. & Wright, W. E. Telomere extension occurs at most chromosome ends and is uncoupled from fill-in in human cancer cells. *Cell* **138**, 463-475 (2009).
9. Hirai, Y., Masutomi, K. & Ishikawa, F. Kinetics of DNA replication and telomerase reaction at a single-seeded telomere in human cells. *Genes Cells* **17**, 186-204 (2012).
10. Lingner, J., Cooper, J. P. & Cech, T. R. Telomerase and DNA end replication: no longer a lagging strand problem. *Science* **269**, 1533-1534 (1995).
11. Chow, T. T., Zhao, Y., Mak, S. S., Shay, J. W. & Wright, W. E. Early and late steps in telomere overhang processing in normal human cells: the position of the final RNA primer drives telomere shortening. *Genes Dev* **26**, 1167-1178 (2012).
12. Yeeles, J. T., Deegan, T. D., Janska, A., Early, A. & Diffley, J. F. Regulated eukaryotic DNA replication origin firing with purified proteins. *Nature* **519**, 431-435 (2015).
13. Yeeles, J. T. P., Janska, A., Early, A. & Diffley, J. F. X. How the Eukaryotic Replisome Achieves Rapid and Efficient DNA Replication. *Mol Cell* **65**, 105-116 (2017).
14. Soudet, J., Jolivet, P. & Teixeira, M. T. Elucidation of the DNA end-replication problem in Saccharomyces cerevisiae. *Mol Cell* **53**, 954-964 (2014).
15. Aria, V. & Yeeles, J. T. P. Mechanism of Bidirectional Leading-Strand Synthesis Establishment at Eukaryotic DNA Replication Origins. *Mol Cell* **73**, 199-211 (2019).
16. Jones, M. L., Aria, V., Baris, Y. & Yeeles, J. T. P. How Pol α-primase is targeted to replisomes to prime eukaryotic DNA replication. *Mol Cell* **in press**,
17. Lim, C. J. & Cech, T. R. Shaping human telomeres: from shelterin and CST complexes to telomeric chromatin organization. *Nat Rev Mol Cell Biol* **22**, 283-298 (2021).
18. Cai, S. W. & de Lange, T. CST–Polα/Primase: the second telomere maintenance machine. *Genes Dev* **in press**,
19. Goulian, M., Heard, C. J. & Grimm, S. L. Purification and properties of an accessory protein for DNA polymerase alpha/primase. *J Biol Chem* **265**, 13221-13230 (1990).

20. Goulian, M. & Heard, C. J. The mechanism of action of an accessory protein for DNA polymerase alpha/primase. *J Biol Chem* **265**, 13231-13239 (1990).
21. Lim, C. J., Barbour, A. T., Zaug, A. J., Goodrich, K. J., McKay, A. E., Wuttke, D. S. & Cech, T. R. The structure of human CST reveals a decameric assembly bound to telomeric DNA. *Science* **368**, 1081-1085 (2020).
22. Lue, N. F. Evolving Linear Chromosomes and Telomeres: A C-Strand-Centric View. *Trends Biochem Sci* **43**, 314-326 (2018).
23. Gao, H., Cervantes, R. B., Mandell, E. K., Otero, J. H. & Lundblad, V. RPA-like proteins mediate yeast telomere function. *Nat Struct Mol Biol* **14**, 208-214 (2007).
24. Miyake, Y., Nakamura, M., Nabetani, A., Shimamura, S., Tamura, M., Yonehara, S., Saito, M. & Ishikawa, F. RPA-like mammalian Ctc1-Stn1-Ten1 complex binds to single-stranded DNA and protects telomeres independently of the Pot1 pathway. *Mol Cell* **36**, 193-206 (2009).
25. Surovtseva, Y. V., Churikov, D., Boltz, K. A., Song, X., Lamb, J. C., Warrington, R., Leehy, K., Heacock, M., Price, C. M. & Shippen, D. E. Conserved telomere maintenance component 1 interacts with STN1 and maintains chromosome ends in higher eukaryotes. *Mol Cell* **36**, 207-218 (2009).
26. Cai, S. W., Zinder, J. C., Svetlov, V., Bush, M. W., Nudler, E., Walz, T. & de Lange, T. Cryo-EM structure of the human CST-Polα/primase complex in a recruitment state. *Nat Struct Mol Biol* **29**, 813-819 (2022).
27. He, Q., Lin, X., Chavez, B. L., Agrawal, S., Lusk, B. L. & Lim, C. J. Structures of the human CST-Polα-primase complex bound to telomere templates. *Nature* **608**, 826-832 (2022).
28. Zaug, A. J., Goodrich, K. J., Song, J. J., Sullivan, A. E. & Cech, T. R. Reconstitution of a telomeric replicon organized by CST. *Nature* **608**, 819-825 (2022).
29. Feng, X., Hsu, S. J., Kasbek, C., Chaiken, M. & Price, C. M. CTC1-mediated C-strand fill-in is an essential step in telomere length maintenance. *Nucleic Acids Res* **45**, 4281-4293 (2017).

30. Takai, H., Jenkinson, E., Kabir, S., Babul-Hirji, R., Najm-Tehrani, N., Chitayat, D. A., Crow, Y. J. & de Lange, T. A POT1 mutation implicates defective telomere end fill-in and telomere truncations in Coats plus. *Genes Dev* **30**, 812-826 (2016).
31. McElligott, R. & Wellinger, R. J. The terminal DNA structure of mammalian chromosomes. *EMBO J* **16**, 3705-3714 (1997).
32. Damm, K., Hemmann, U., Garin-Chesa, P., Hauel, N., Kauffmann, I., Priepke, H., Niestroj, C., Daiber, C., Enenkel, B., Guilliard, B., Lauritsch, I., Müller, E., Pascolo, E., Sauter, G., Pantic, M., Martens, U. M., Wenz, C., Lingner, J., Kraut, N., Rettig, W. J. & Schnapp, A. A highly selective telomerase inhibitor limiting human cancer cell proliferation. *EMBO J* **20**, 6958-6968 (2001).
33. Larrivée, M., LeBel, C. & Wellinger, R. J. The generation of proper constitutive G-tails on yeast telomeres is dependent on the MRX complex. *Genes Dev* **18**, 1391-1396 (2004).
34. Baird, D. M., Rowson, J., Wynford-Thomas, D. & Kipling, D. Extensive allelic variation and ultrashort telomeres in senescent human cells. *Nat Genet* **33**, 203-207 (2003).
35. Anderson, B. H., Kasher, P. R., Mayer, J., Szynkiewicz, M., Jenkinson, E. M., Bhaskar, S. S., Urquhart, J. E., Daly, S. B., Dickerson, J. E., O'Sullivan, J., Leibundgut, E. O., Muter, J., Abdel-Salem, G. M., Babul-Hirji, R., Baxter, P., Berger, A., Bonafé, L., Brunstom-Hernandez, J. E., Buckard, J. A., Chitayat, D., Chong, W. K., Cordelli, D. M., Ferreira, P., Fluss, J., Forrest, E. H., Franzoni, E., Garone, C., Hammans, S. R., Houge, G., Hughes, I., Jacquemont, S., Jeannet, P. Y., Jefferson, R. J., Kumar, R., Kutschke, G., Lundberg, S., Lourenço, C. M., Mehta, R., Naidu, S., Nischal, K. K., Nunes, L., Ounap, K., Philippart, M., Prabhakar, P., Risen, S. R., Schiffmann, R., Soh, C., Stephenson, J. B., Stewart, H., Stone, J., Tolmie, J. L., van der Knaap, M. S., Vieira, J. P., Vilain, C. N., Wakeling, E. L., Wermenbol, V., Whitney, A., Lovell, S. C., Meyer, S., Livingston, J. H., Baerlocher, G. M., Black, G. C., Rice, G. I. & Crow, Y. J. Mutations in CTC1, encoding conserved telomere maintenance component 1, cause Coats plus. *Nat Genet* **44**, 338-342 (2012).

36. Takai, H., Xie, Y., de Lange, T. & Pavletich, N. P. Tel2 structure and function in the Hsp90-dependent maturation of mTOR and ATR complexes. *Genes Dev* **24**, 2019-2030 (2010).
37. Komura, J. & Riggs, A. D. Terminal transferase-dependent PCR: a versatile and sensitive method for in vivo footprinting and detection of DNA adducts. *Nucleic Acids Res* **26**, 1807-1811 (1998).
38. Hanish, J. P., Yanowitz, J. L. & de Lange, T. Stringent sequence requirements for the formation of human telomeres. *Proc Natl Acad Sci U S A* **91**, 8861-8865 (1994).
39. Harley, C. B., Futcher, A. B. & Greider, C. W. Telomeres shorten during ageing of human fibroblasts. *Nature* **345**, 458-460 (1990).
40. Smogorzewska, A., Karlseder, J., Holtgreve-Grez, H., Jauch, A. & de Lange, T. DNA ligase IV-dependent NHEJ of deprotected mammalian telomeres in G1 and G2. *Curr Biol* **12**, 1635-1644 (2002).

Figure legends

Figure 1. In vitro replication of linear templates reveals a second end-replication problem.

a, Schematic of the end-replication problem at a telomere with a 100 nt 3´ overhang and its solution by telomerase prior to this study (modified from refs. 7 and 10[7,10]). ***b***, Schematic of the in vitro replication approach to determine the replisome products DNA ends. ***c***, Diagrams of replication templates and anticipated leading and lagging-strand products. The location of the BbvCI site and the anticipated products of nicking by Nb.BbcvCI and Nt.BbvCI are shown. ***d***, Denaturing 8% polyacrylamide/urea gel analysis of a replication reaction performed on the templates illustrated in (**c**). Products were

post-replicatively digested with Nt./Nb.BbvCI as indicated. ***e***, Lane profiles of the data in (**d**). ***f***, Schematic illustrating that the last Okazaki fragment starts >40 nt from the 5´ end of the template and the terminal structures predicted to be created by replication of a linear DNA.

Figure 2. C-strand loss at leading- and lagging-end telomeres in absence of CST

a, Immunoblot for Ctc1 in CTC1$^{F/F}$ HCT116 cells (plus and minus Cre) after bulk knockout of hTERT (sgTERT). sgLuc: Luciferase control. ***b***, TRAP assay on extracts from the cells in (**a**). 250H: Heat-inactivated extract (250 cells). Cntrl: positive control. I: internal PCR control. ***c***, In-gel overhang assay for relative overhang signals of leading- (lead) and lagging- (lag) end telomeres in telomerase-deficient CTC1$^{F/F}$ cells as in (**b**). BrdU-labelled leading- and lagging-end telomeres were isolated on CsCl gradients. Left: hybridization with TelC to detect the G-strand overhang. Right: same gel, reprobed with TelC after in situ denaturation, detecting total telomeric DNA for normalization (normalized values relative to lane 1). Cells were harvested at PD 5 after Ctc1 deletion. ***d***, Graph showing the relative overhang signals and SDs from six independent experiments as in (**c**). P values determined by paired t-test. ***e***, Overhang PCR products (Method I) from cells (CTC1$^{F/F}$/no 4-OHT) with and without telomerase. Four parallel PCR reactions for each DNA sample are loaded. Calculated 3´ overhang lengths are on the left. ***f***, Graph showing average 3´ overhang lengths and SDs from 4 biological replicates (4 PCR reactions/replicate) as in (**e**). ns, not significant based on paired t-test. ***g***, Analysis of 3´ overhang lengths using Method II. DNA from cells as in (**e**) were ExoI- (or mock-) treated and denatured, MboI/AluI digested fragments were fractionated on an

alkaline agarose gel. Shortening of G-strands was detected by in-gel hybridization with TelC. ***h***, Graph showing average 3´ overhang lengths and SDs determined by Method II on 4 biological replicates as in (**g**). ***i***, Absolute overhang lengths at leading- and lagging-end telomeres in telomerase-deficient cells with and without Ctc1. The values with asterisks were measured and used to calibrate the relative overhang values in (**d**). ***j***, C-strand loss in cells lacking Ctc1 and telomerase based on (***i***) and Extended Data Fig. 5.

Figure 3. Without CST telomeric overhangs increase at the predicted rate

a, Schematic of the predicted C-strand sequence loss at leading- and lagging-end telomeres in telomerase- and Ctc1-deficient cells based on the 3´ overhang lengths measured in Figure 2. The predicted relative overhang change (black) was calculated based on the initial overhang length (82 nt) and changes of predicted overhang at lagging- (red) and leading- (green) ends. ***b***, In-gel overhang assays on telomerase-deficient (sgTERT/BIBR1532) CTC1$^{F/F}$ cells (with or without 4-OHT Cre induction). Relative normalized overhang signals are given below the gel with the first lane set to 1. ***c***, Graph showing close agreement with the predicted (as in panel a) and observed 3´ overhang changes. Values are from 3 independent experiments as in (**b**) with SDs shown.

Figure 4. C-strand shortening at the predicted rate in absence of CST.

a, Immunoblot for Ctc1 in CTC1$^{F/F}$ HCT116 cells with and without induction of Cre with 4-OHT. Ctrl: non-specific band serving as a loading control. ***b***, Alkaline agarose gel analysis of the G- and C-strand of telomeric fragments in telomerase proficient CTC1$^{F/F}$

cells after with/without 4-OHT induction of Cre. Left: in-gel hybridization with TelC probe to detect the G-strands. Right, duplicate gel probed with TelG to detect the C-strands. ***c***, Graph showing the changes in length of the G- and C-strands as determined in (**b**). ***d***, Close agreement of the observed length changes in Ctc1-deficient cells with calculated length changes based on C-strand shortening of 84 nt/PD and G-strand elongation of 200 nt/PD by telomerase. ***e***, Schematic illustrating the two end-replication problems. The leading-end replication problem is solved by telomerase elongating the G-rich strand. CST–Polα-primase provides the solution to the lagging-strand replication problem which results the position of the last Okazaki fragment synthesized by the replisome. In addition, CST–Polα-primase makes up for the C-strand sequence loss resulting from 5´ end resection.

Figure 1. Takai, Aria et al.

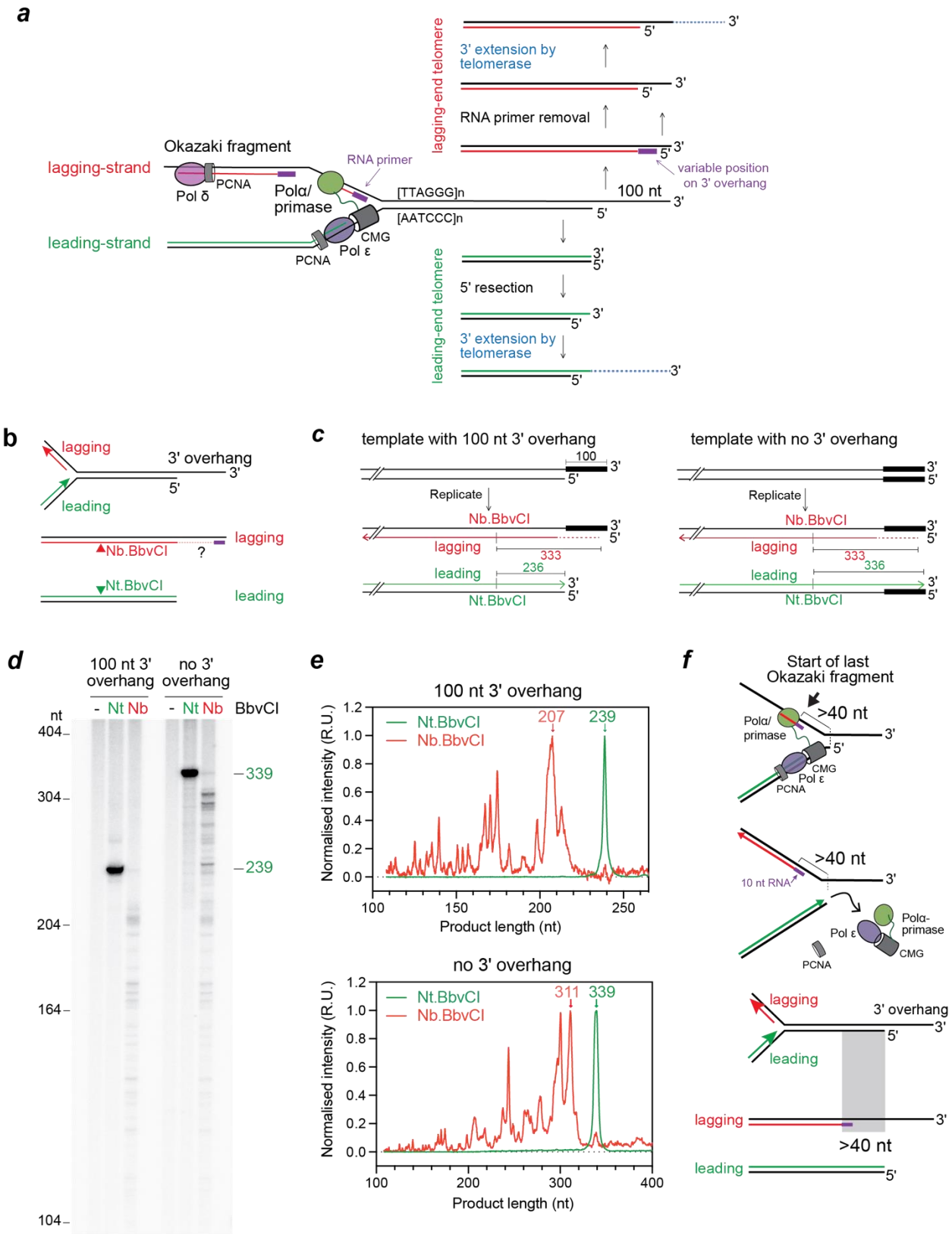

Figure 2. Takai, Aria et al.

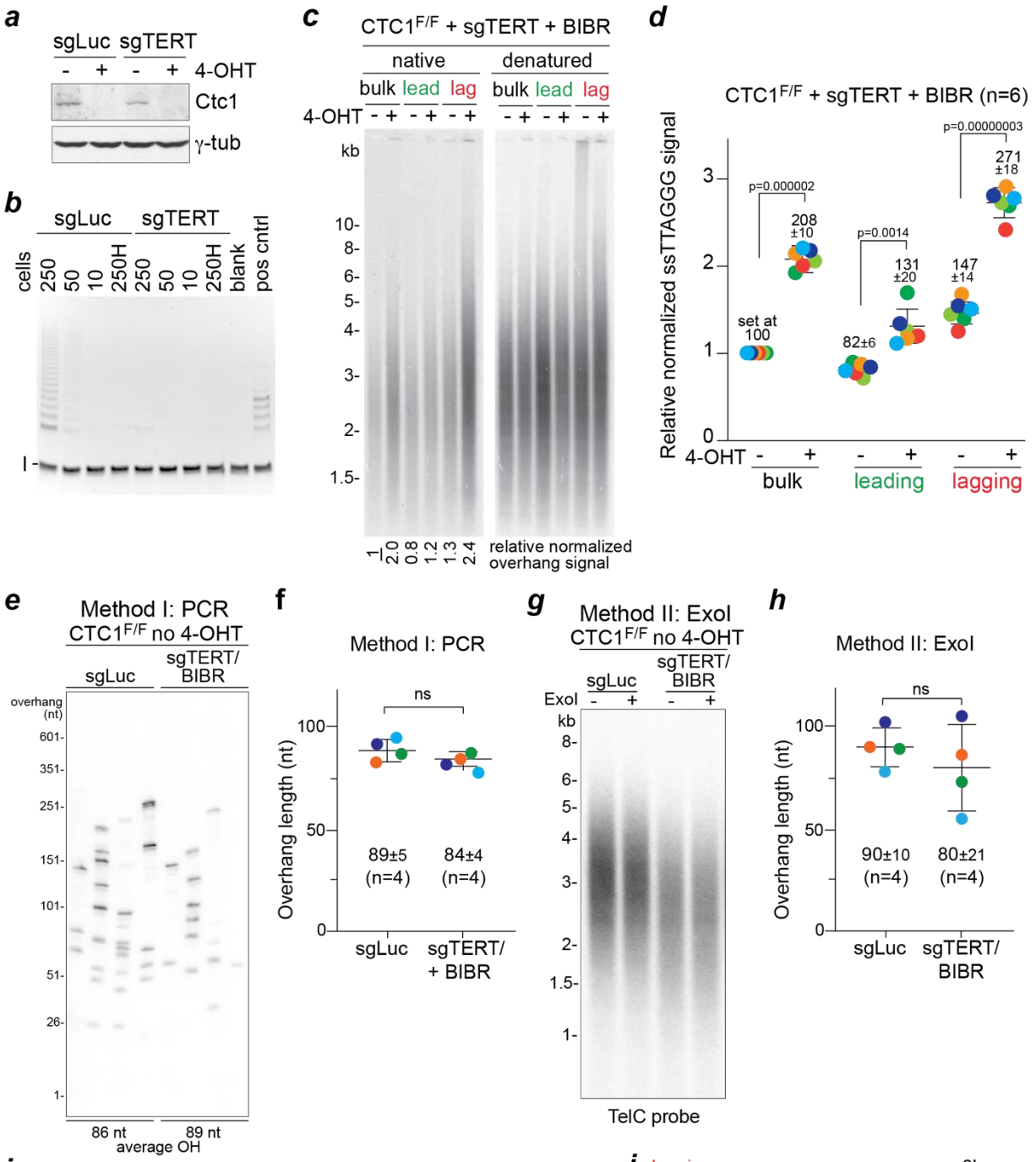

	CTC1F/F + sgTERT/BIBR at PD 5					
	no 4-OHT			+ 4-OHT		
	3' overhang length (nt)			3' overhang length (nt)		
	bulk	leading	lagging	bulk	leading	lagging
Method I	84 ±4	69 ±5	124 ±12	175 ±8	110 ±17	228 ±15
Method II	80 ±21	66 ±5	117 ±11	166 ±8	105 ±16	217 ±14
Average	82	68	121	171	108	223

Figure 3. Takai, Aria et al.

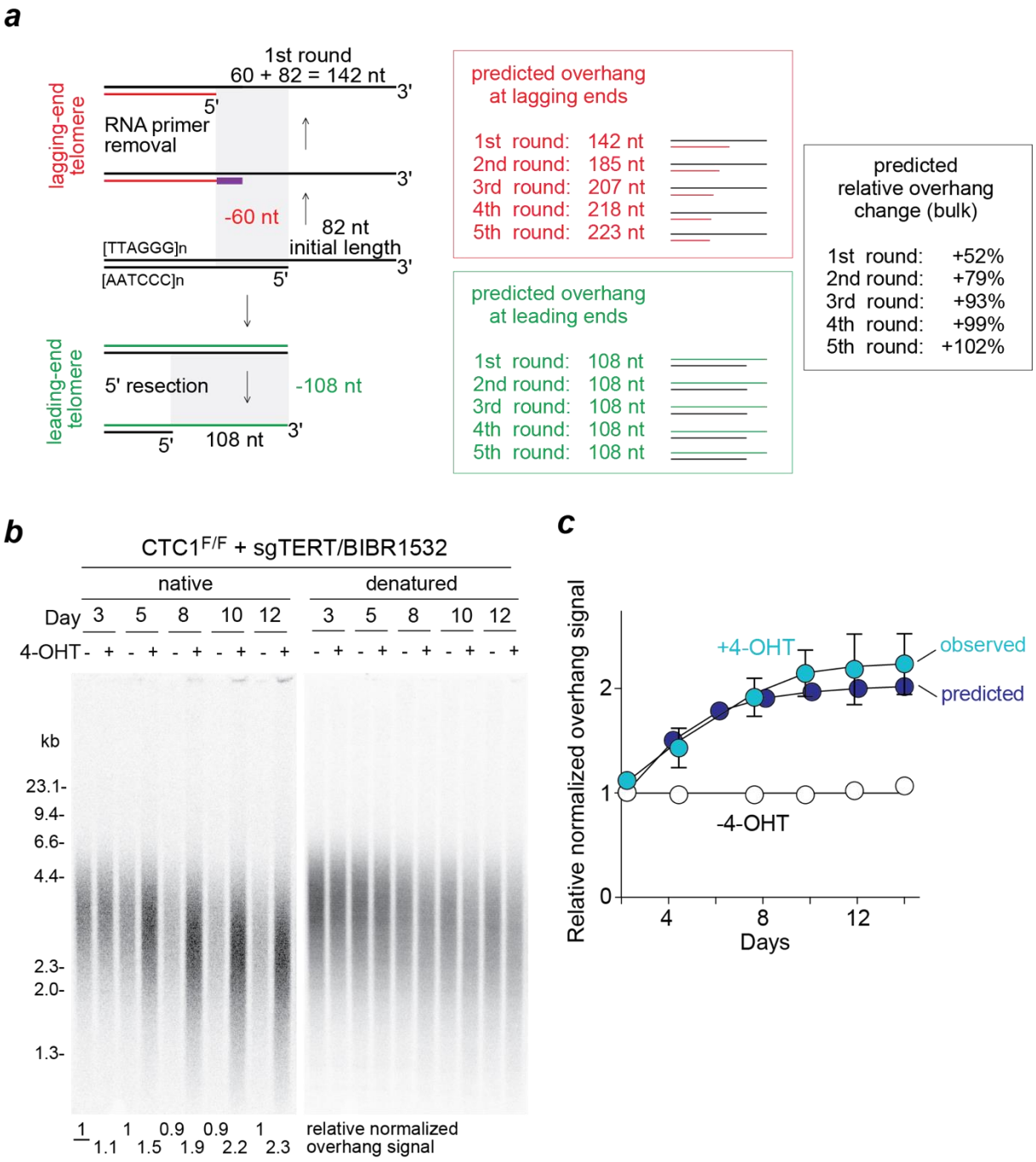

Figure 4. Takai, Aria et al.

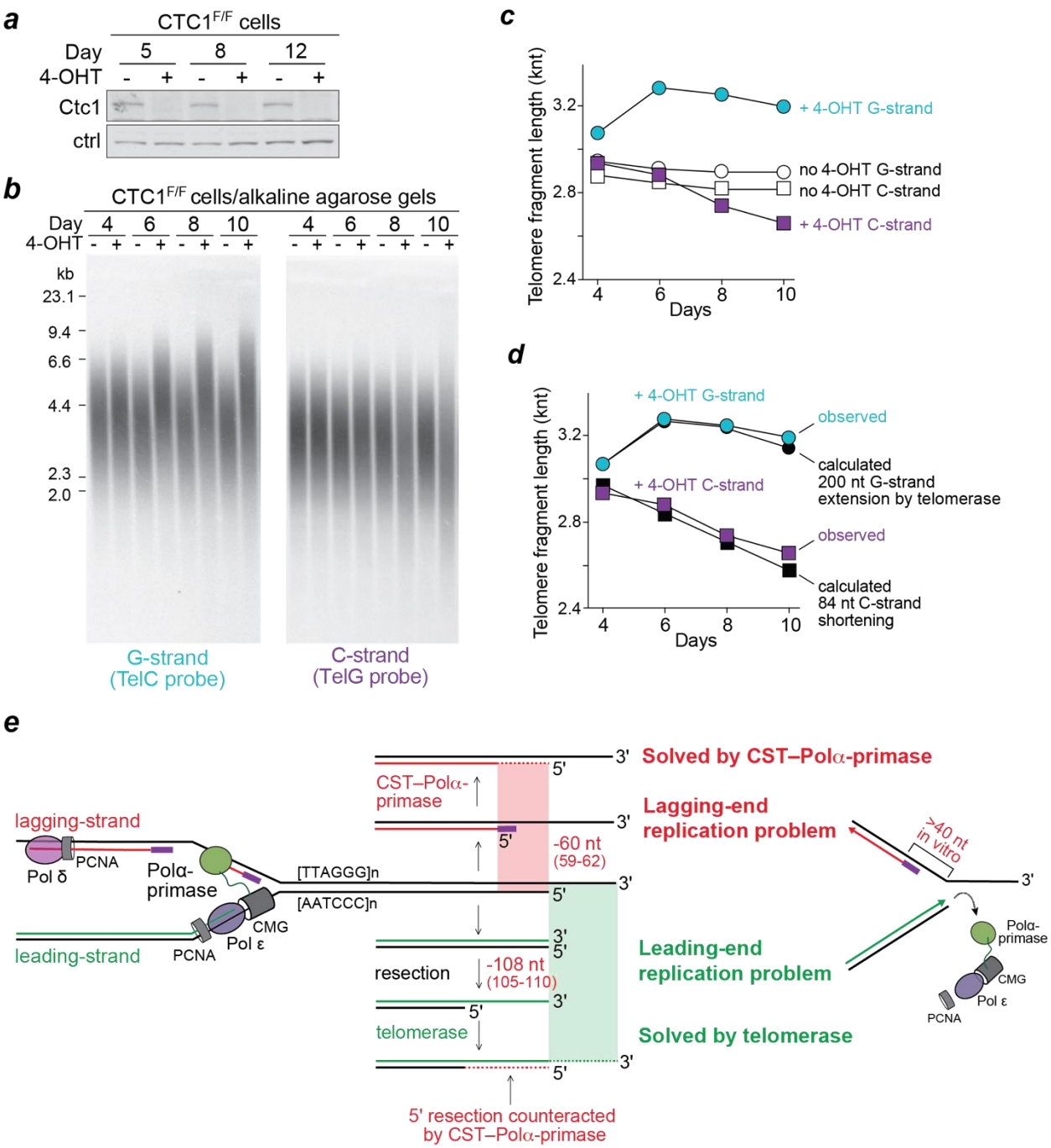

Extended Data

Extended Data Figure 1. RNAse HII digestion of the lagging-strand products replication products

a, Denaturing 8% polyacrylamide gel analysis of a replication reaction performed on the no overhang template illustrated in panel c of Figure 1. Products were post-replicatively digested with Nt./Nb.BbvCI and RNAse HII as indicated. Lane profiles of the data are given next to the gels. ***b***, As in (**a**) but using the 3´ overhang template. ***c***, Comparison of Polα-primase in the yeast and human replisomes. For clarity only Polα-primase, CMG and DNA are shown. The shortest distance between the point of strand separation and the primase active site are illustrated (dashed red line).

Extended Data Figure 2. CsCl-gradient separation of leading- and lagging-end telomeres.

a, Schematic of the experimental approach. ***b***, Examples of slot blots to detect telomeric DNA in fractions from CsCl gradients. Pooled fractions used for in-gel 3´ overhang assays are indicated at the top.

Extended Data Figure 3. Validation of the PCR overhang assay (Method I)

a, Schematic of the PCR assay for telomeric overhangs. Genomic DNA is poly(A) tailed and annealed to 5´ biotinylated oligo(dT) primers containing the teltail sequence and 4 nt telomeric C-strand sequence (in all six frames). After a primer extension reaction, DNAs are digested with AluI, fractionated by molecular size to remove primers and

small DNA fragments, captured on Streptavidin beads, denatured, and neutralized. The DNAs on the beads tailed with rGTP, ligated to a PCR adapter containing 3´ G-strand nucleotides in all six frames and amplified with the indicated primers. PCR products are separated on polyacrylamide/urea gels, blotted, and hybridized with telomeric G-strand probe. ***b***, Schematic of the telomere model substrate generated by ligating a telomeric 3´ overhang to a HindIII/BglII fragment of pSXneo1.6T2AG3. ***c***, PCR overhang assay on the model telomeric substrate with and without *E. coli* ExoI treatment to remove the overhang. ***d***, PCR overhang assay on genomic DNA with and without pre-treatment with ExoI showing the specificity of the assay for 3´ overhangs. Average sizes of 3´ overhangs are given below the panel. ***e***, PCR overhang assay detects elongated 3´ telomeric overhang in cells lacking Ctc1. PCR overhang assays were performed using DNA from CTC1$^{F/F}$ cells with or without 4-OHT treatment for 10 days. The length of the overhangs in the Ctc1-deficient cells in an estimate since the reliability of the assay in that size range is not known. ***f***, PCR overhang assays performed with synthetic telomeric oligos containing 5 to 20 TTAGGG repeats. Tel10 -Lig: Tel10 oligo processed in parallel but without ligation to the adaptor. ***g***, Relative signal intensity of 6 independent PCR overhang assays as in (**f**) were plotted. The signal intensity of Tel5 oligo in each experiment was set at 1. ***h***, In-gel hybridization assay showing that telomerase expression does not affect the 3´ overhang length when CST is present. Genomic DNAs from CTC1$^{F/F}$ cells with or without sgTERT/BIBR treatment were treated with *E. coli* ExoI as indicated and MboI/AluI digested DNA was separated in agarose gel. Left: TelC probe detecting the overhang signals. Right: same gel probed with TelC after in situ denaturation to detect the total telomeric DNA for normalization.

Extended Data Figure 4. Validation of overhang measurement using ExoI (Method II)

a, Telomere model substrate with or without overhang shown in Ext. Data Fig. 3b was treated with or without ExoI and applied for agarose alkaline gel electrophoresis and detected by in-gel hybridization with the TelC probe. Size of the detected fragments was was calculated based on the molecular weight marker. Shortening of the model telomere substrate G-strand by ExoI is shown below the gel. ***b***, Telomeric signals obtained by in-gel hybridization to alkaline agarose gels as shown in Fig. 2g were scanned and plotted as line graphs using Fiji software (Image J, ver2) and superimposed. ***c***, Mobility of DNA molecular marker at the left and right sides of the alkaline agarose gel used to convert the line graphs in (**b**) to telomere lengths.

Extended Data Figure 5. Inferred C-strand shortening at lagging-end telomeres

a, Schematic showing the changes at leading- and lagging-end telomeres over three rounds of replication in cells lacking Ctc1 and telomerase. Resection of the leading-end products was set at 108 nt (Fig. 2j). Sequence loss at the lagging-end C-strand is inferred to be 60 nt based on the value of 223 nt (average of 228 and 217) for lagging-end telomeres (Fig. 2j). ***b***, Equation for C-strand loss at lagging-end telomeres with cell divisions. ***c***, Overhang lengths predicted in 5 successive rounds of replication as depicted in (**a**). Note that the value for the lagging-end overhangs is predicted to plateau (at ~185 nt) as observed in Fig. 3c.

Extended Data Figure 6. C-strand shortening in HCT116 cells lacking Ctc1.

a-c, Measurement of C-strand shortening CTC1$^{F/F}$ cells with or without 4-OHT treatment based on alkaline gel analysis of the telomeric G- and C-strands. See Fig. 4b-d for methods and details.

Extended Data Figure 7. Schematic illustrating the dynamics of the C- and G-strand in Ctc1-deficient cells expressing telomerase.

a, Schematic showing the changes of G- and C-strand telomere length over three rounds of replication in telomerase-proficient cells lacking Ctc1. G-strand sequences added by telomerases are depicted with a blue line. The numbers given are as follows (based on Fig. 2i and Extended Data Fig. 5). *X*: nucleotides added by telomerase; 82 nt: initial 3´ overhang length; 60 nt: loss of sequences due to incomplete lagging-strand synthesis; 108 nt: resection of the C-strand at leading-end telomeres. ***b***, Equation describing changes in average G-strand length after each round of replication (n) relative to initial G-strand telomere length. ***c***, Increase in average G-strand length with cell divisions calculated using the equation in (b) and assuming that telomerase adds an average of 200 nt (*X*) to each end. ***d***, Modeled changes in the length of the G-strand in Ctc1-deficient cells based on the initial G-strand length of 3.07 kb. To determine *X*, the value for telomerase extension was increased stepwise by 10 nt, plotted and the plot was compared to the actual G-strand changes obtained in Fig. 4d. When *X* is 200 nt, the model plot is a close fit with the *in vivo* data as shown in Fig. 4d.

Ext. Data Fig. 1. Takai, Aria et al.

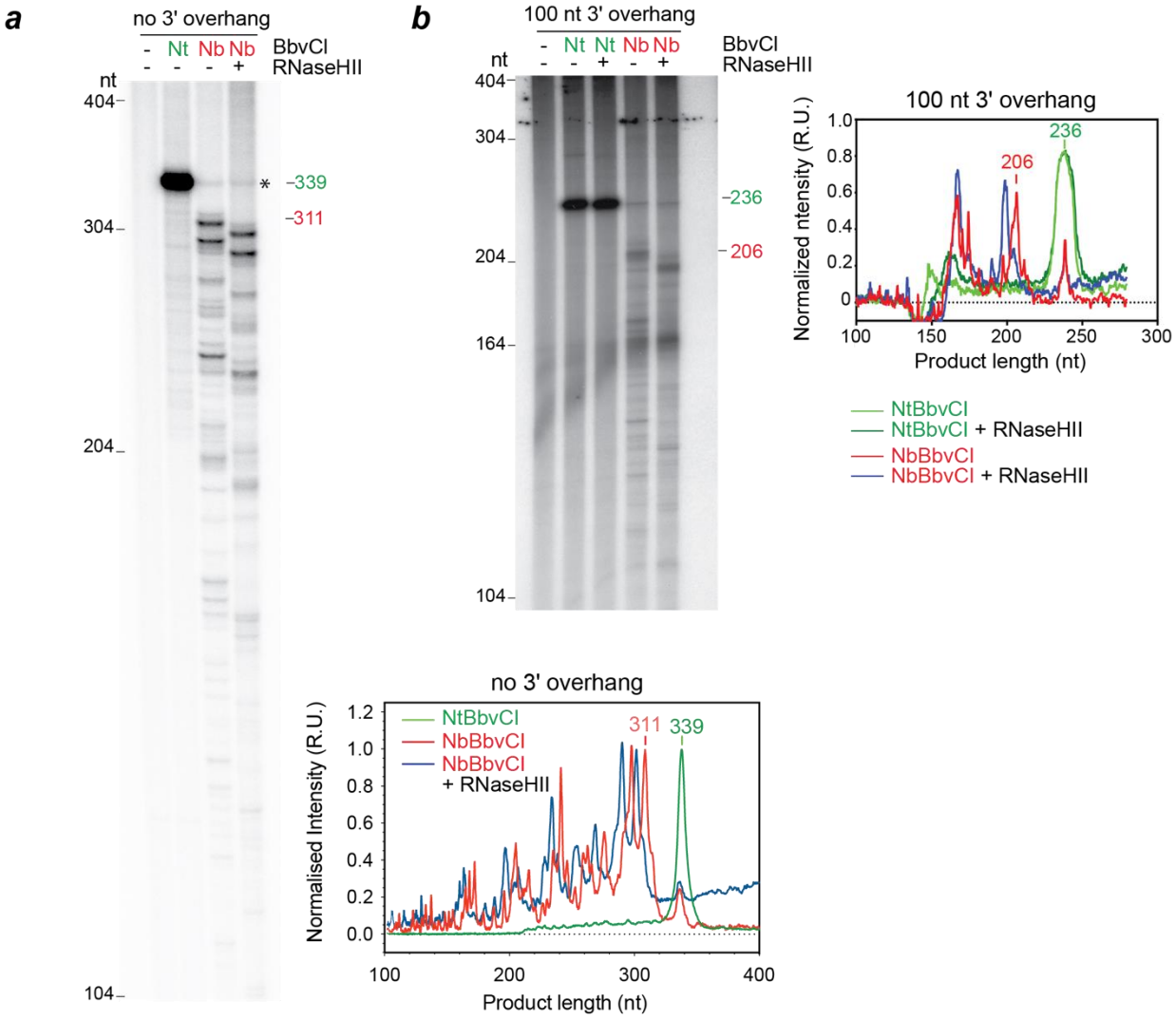

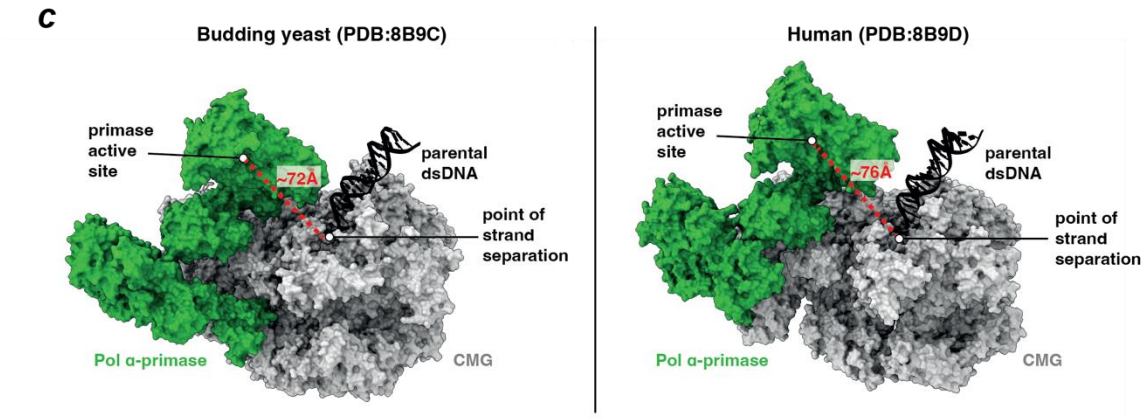

Ext. Data Fig. 2. Takai, Aria et al.

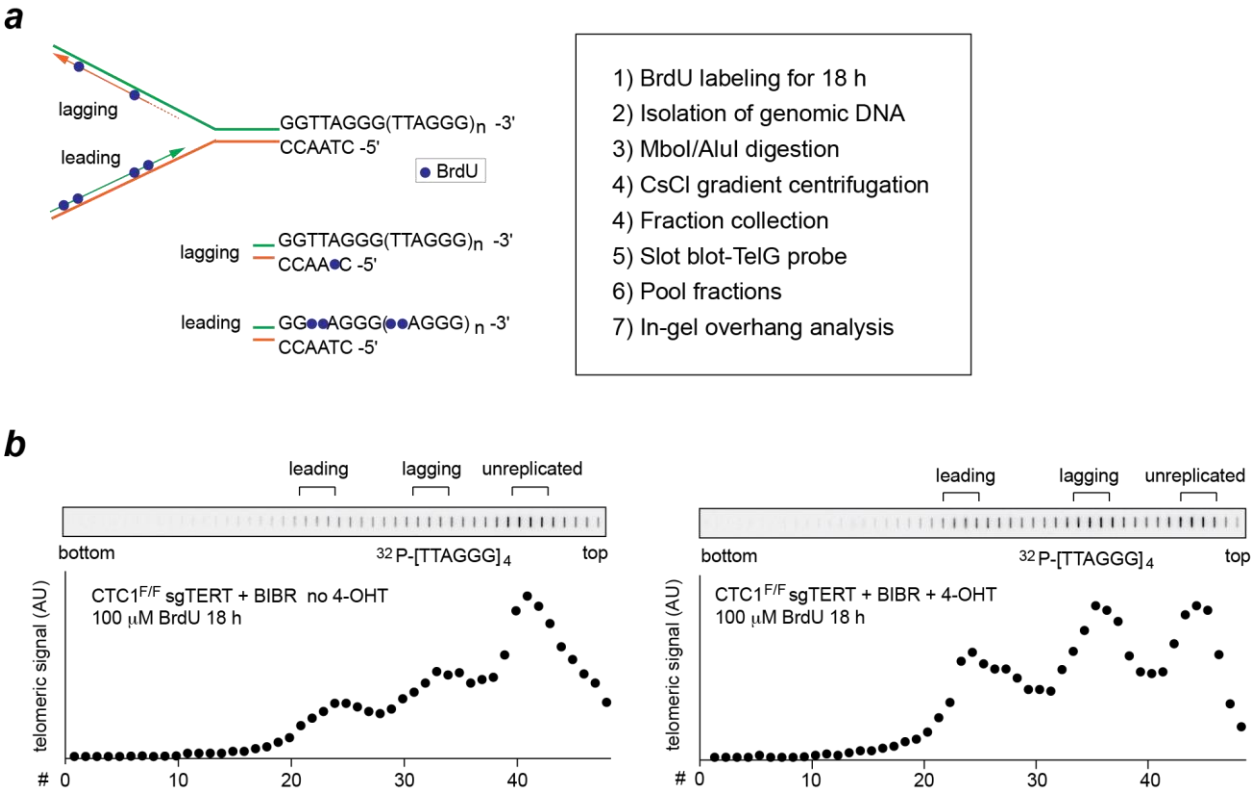

Ext. Data Fig. 3. Takai, Aria et al.

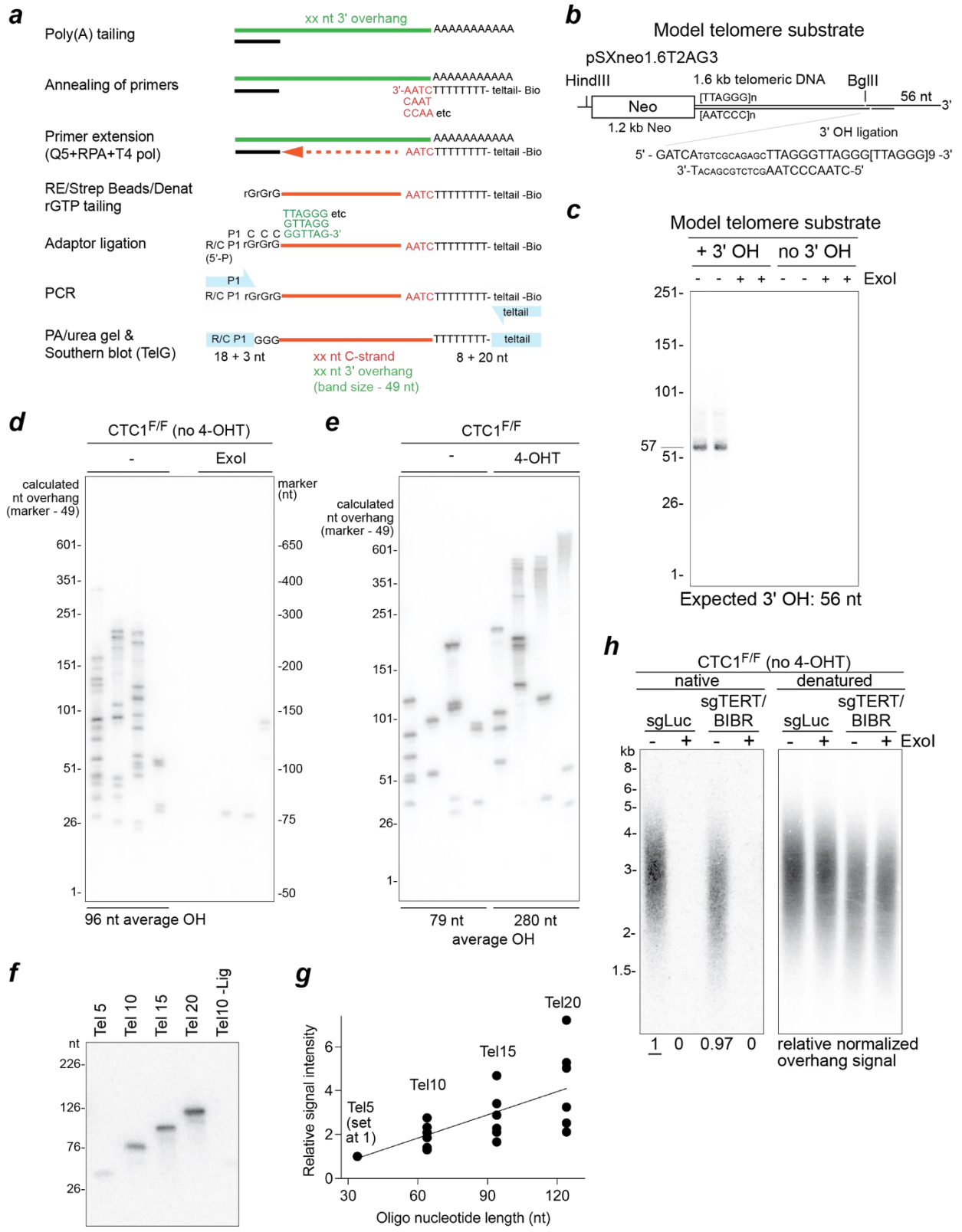

Ext. Data Fig. 4. Takai, Aria et al.

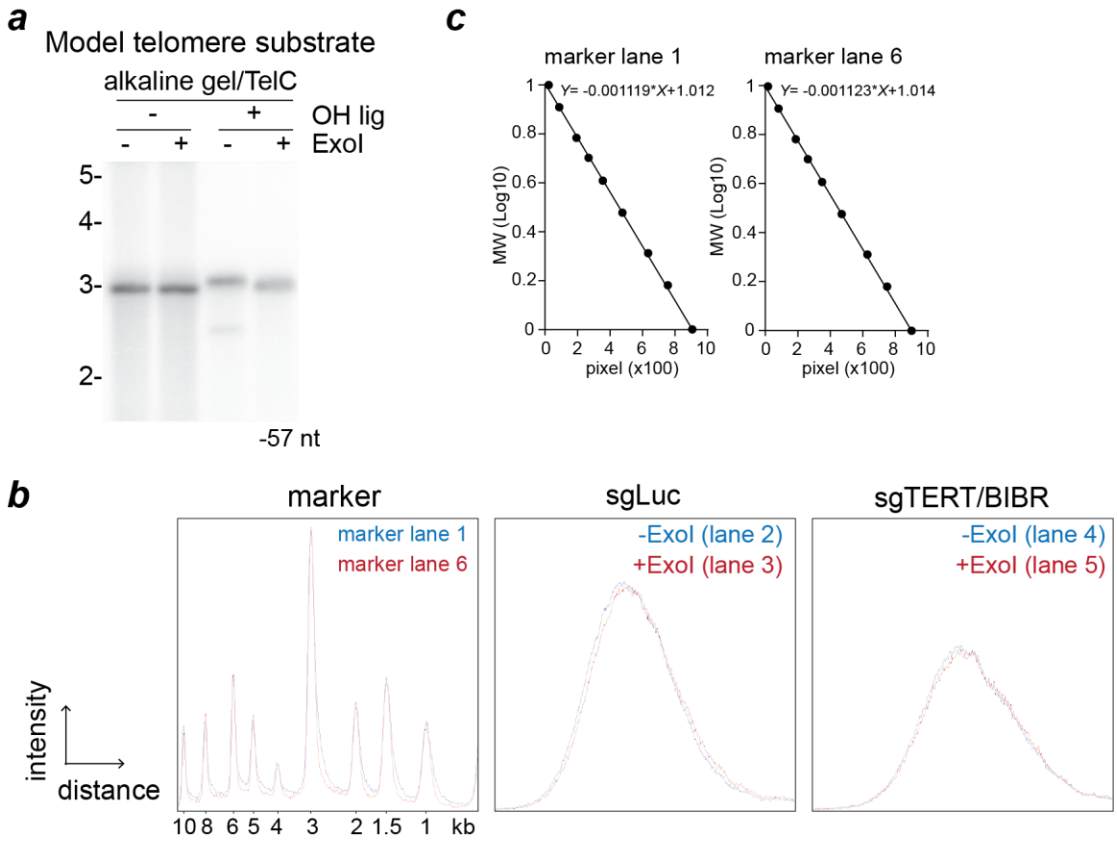

Ext. Data Fig. 5. Takai, Aria et al.

a

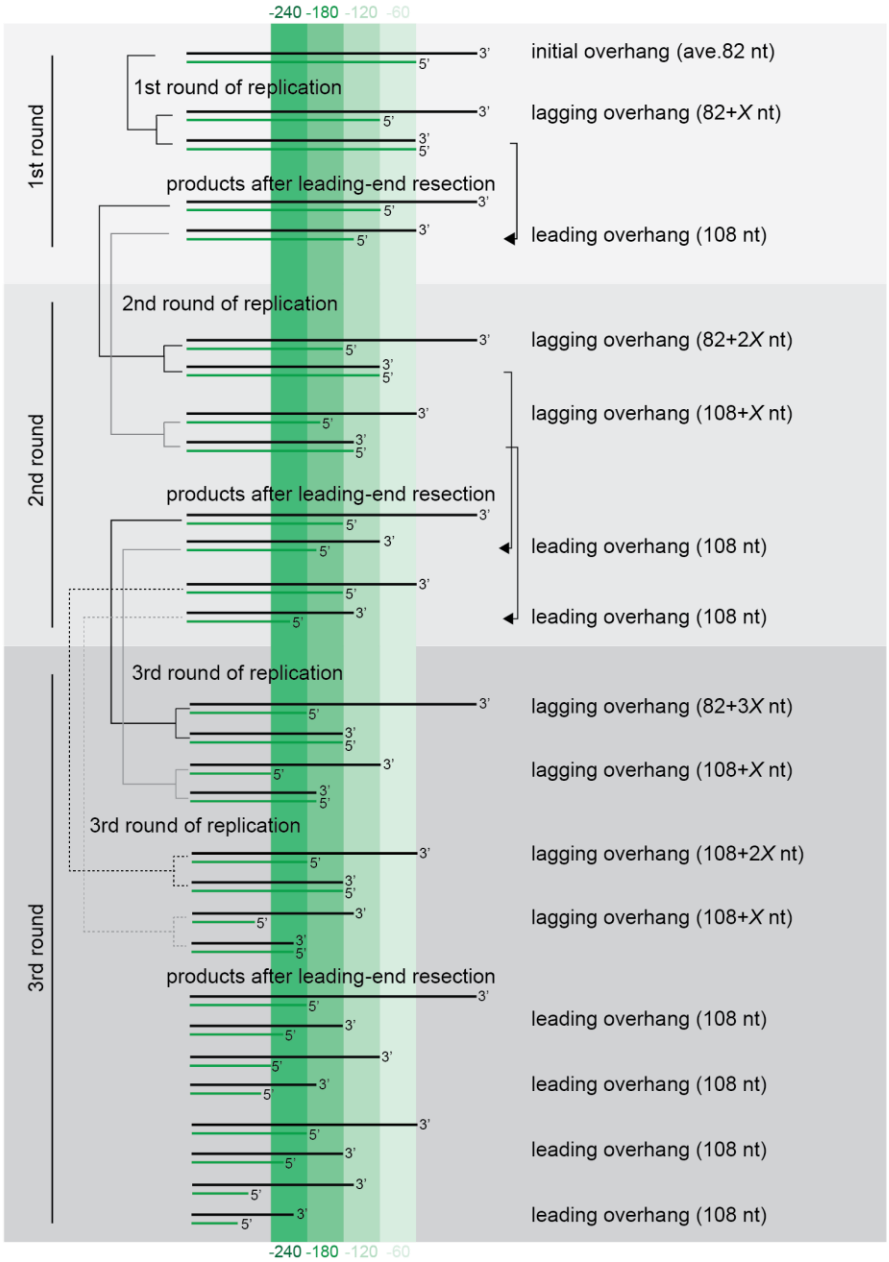

b

$$\frac{F_{lag} + R_{lead}}{2} = \frac{(2^{D\#} - 1)X + Y + (2^{D\#} - 1)R_{lead}}{2^{D\#}}$$

When $D\#$=5 and F_{lag} =223, X=60

Y = initial overhang length (82 nt)
$D\#$ = rounds of replication
R_{lead} = resection at leading ends (108 nt)
F_{lag} = length of lagging OH after $D\#$
X = loss at lagging end/cell division

c

Predicted average 3' overhang length

lagging strand	leading strand	both
1st round: 142 nt	1st round: 108 nt	1st round: 125 nt
2nd round: 185 nt	2nd round: 108 nt	2nd round: 147 nt
3rd round: 207 nt	3rd round: 108 nt	3rd round: 158 nt
4th round: 218 nt	4th round: 108 nt	4th round: 163 nt
5th round: 223 nt	5th round: 108 nt	5th round: 166 nt

Ext. Data Fig. 6. Takai, Aria et al.

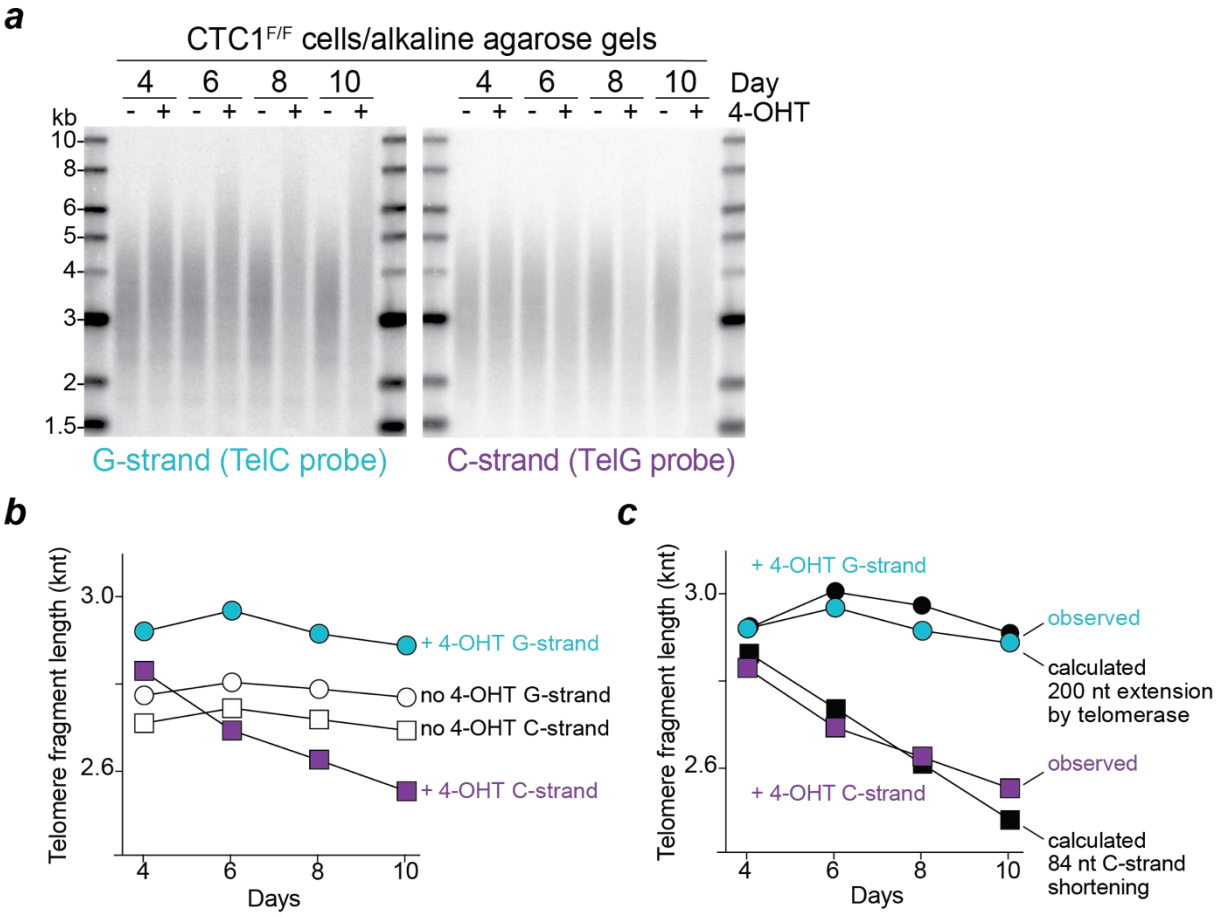

Ext. Data Fig. 7. Takai, Aria et al.

a

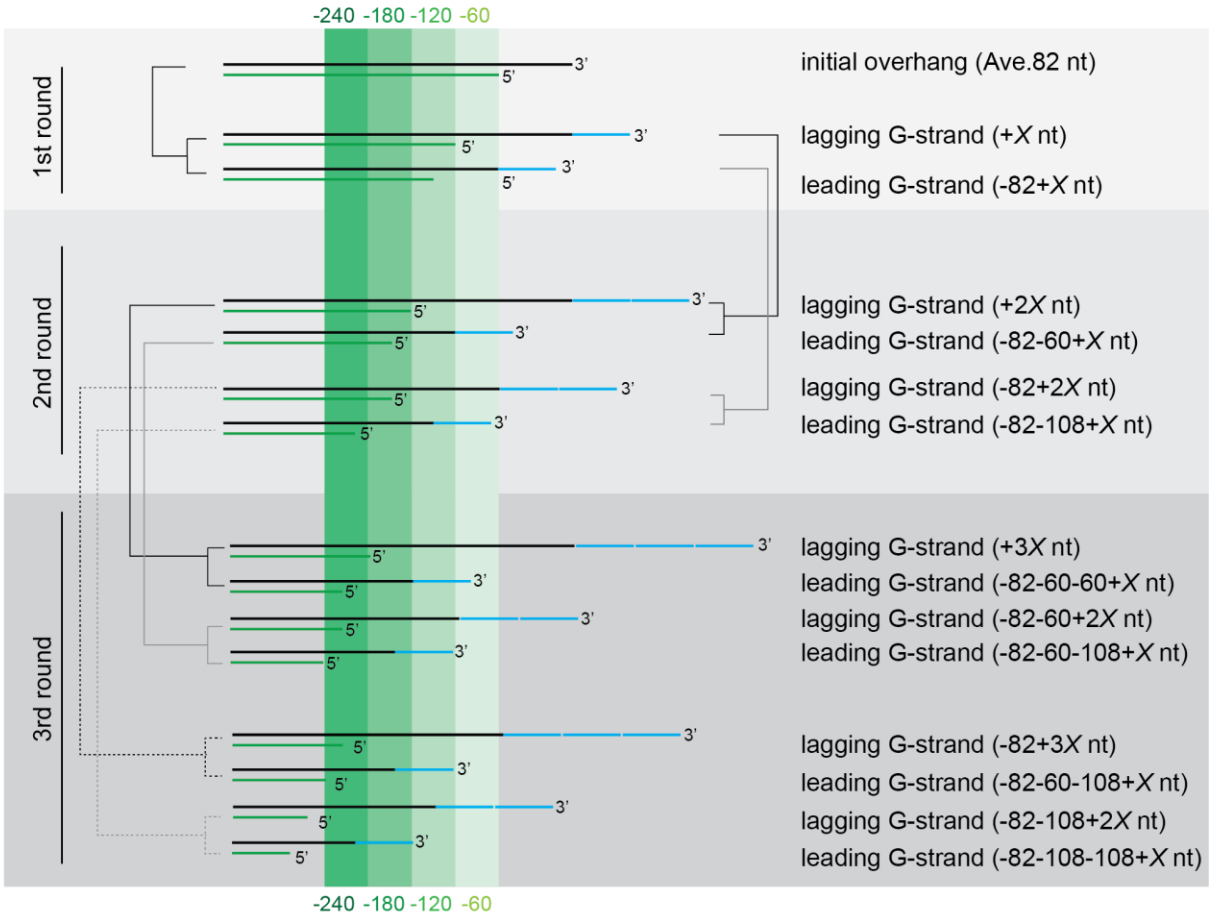

b

$$\frac{1}{2^n}\sum_{k=1}^{n}\{[-Y-\frac{Rlag+Rlead}{2}(k-1)]2^{k-1}+2^kX\}$$

n; cell division number,
Rlag; C-strand shortening at lagging strands (60 nt),
Rlead; C-strand shortening at leading strands (108 nt),
Y; initial 3' overhang (82 nt)
X; G-strand elongation by telomerase (nt)/cell division

c

Average change of G-strand length after the indicated rounds of replication w/o Ctc1 (assuming *X*=200)	
1st round:	+159
2nd round:	+196
3rd round:	+173
4th round:	+119
5th round:	+51
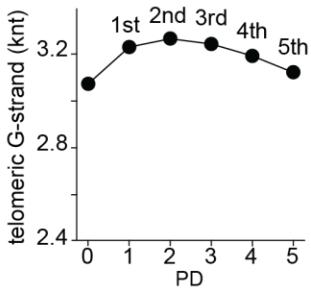
d